Pergamon

PII: S0277-5387(97)00111-3

Polyhedron Vol. 16, No. 18, pp. 3235–3246, 1997

0277-5387/97 $17.00+0.00

Mechanism and kinetics of hydrodenitrogenation

R. Prins,* M. Jian and M. Flechsenhar

Laboratory for Technical Chemistry, Federal Institute of Technology (ETH), 8092 Zürich, Switzerland

Abstract—Removal of the nitrogen atom from aromatic nitrogen-containing molecules takes place *via* hydrogenation of the aromatic rings, C—N bond cleavage of the resulting saturated amines by NH_3 elimination, and alkene (de)hydrogenation. The separate reaction steps cannot be combined into one kinetic equation, because every reaction takes place on a different catalytic site which differs in its ability to bind reactants, intermediates and products. A multi-site Langmuir–Hinshelwood rate model has to be used in the kinetic modeling. Depending on the type of molecule, aniline or pyridine-like, the rate determining step is phenyl hydrogenation or ring opening elimination, respectively. The HDN behaviour of polycyclic aromatic N-containing molecules is based on a combination of the HDN reactions of aniline and pyridine-like molecules.

The catalyst components influence the rate as well as the adsorption constants. Ni has a positive effect on all reactions steps for all reactant molecules, while the effect of phosphorus depends on the type of rate determining reaction, and thus on the reactant. Hydrogenation reactions are promoted by P (aniline and alkene), and elimination reactions are negatively influenced (piperidine and decahydroquinoline). The reverse is true for H_2S, suggesting that phosphorus increases the number of sulfur vacancies which are considered to be the catalytic sites for (de)hydrotreating reactions. © 1997 Elsevier Science Ltd

Keywords: hydrodenitrogenation; kinetics; mechanism.

Polycyclic aromatic nitrogen compounds such as quinoline and indole, and sulfur compounds such as benzothiophene are the main nitrogen and sulfur-containing compounds in oil fractions. They must be removed by so-called hydrotreating processes, because the burning of oil fractions in engines and factories would otherwise lead to air-polluting emissions of nitrogen and sulfur oxides. Furthermore, many catalysts which are used for the processing of oil fractions cannot tolerate sulfur and metals, and most oil streams in a refinery must therefore by hydrotreated. As a consequence, hydrotreating is the largest application of industrial catalysis on the basis of the amount of material processed per year, and hydrotreating catalysts constitute the third largest catalyst business after exhaust gas catalysts and fluid cracking catalysts, based on the amount of catalyst sold per year.

Because of the aromaticity of the nitrogen-containing ring in polycyclic aromatics, the nitrogen atom can only be removed after hydrogenation of this ring and this requires relatively high H_2 pressures. Polycyclic N-containing aromatics have a carbocyclic as well as a heterocyclic ring, and therefore there are two ways to remove the nitrogen atom from such molecules: One route goes *via* aniline-type molecules, and the other *via* pyridine and piperidine-like molecules. In the following we will describe how kinetic studies contribute to the understanding of the mechanisms of the hydrodenitrogenation (HDN) reactions of these two classes of molecules, and how this can be used to understand the HDN of larger molecules such as quinoline. As model compound for the aniline class of molecules we have taken ortho-propylaniline, while 5,6,7,8-tetrahydroquinoline and decahydroquinoline were taken as representatives from the pyridine and piperidine-type compounds. All three compounds are intermediates in the HDN of quinoline. But before discussing the kinetic and mechanistic results, the structure of a working, a sulfided catalyst will be described in the next section, in order to provide a background against which the mechanisms and kinetics can be appreciated.

CATALYST STRUCTURE

Hydrotreating catalysts contain molybdenum and cobalt or nickel, supported on γ-Al_2O_3 [1,2]. Cobalt

* Author to whom correspondence should be addressed.

is mainly used in hydrodesulfurization (HDS), while nickel is favoured in hydrodenitrogenation (HDN). In addition to Mo and Co or Ni, hydrotreating catalysts often contain modifier elements, such as P, B, F, or Cl, which may influence the catalytic as well as the mechanical properties of the catalyst.

Hydrotreating catalysts are prepared in two steps. First, oxidic catalyst precursors are formed by impregnation of the alumina support with aqueous solutions of Mo and Co or Ni salts, and subsequent drying and heating in air. Second, these catalysts precursors are transformed into the actual hydrotreating catalysts by sulfidation in a mixture of H_2 and a sulfur-containing molecule like H_2S or dimethyldisulfide. During sulfidation, as well as during actual hydrotreating, the conditions are highly reducing with H_2S always present, and thermodynamics predict that molybdenum should be in the MoS_2 form. Indeed, Extended X-ray Absorption Fine Structure (EXAFS) studies of Mo K-edge absorption spectra demonstrated that in sulphided Mo/Al_2O_3 catalysts the average Mo ion has the same environment as a Mo ion in MoS_2 [3–5]. The only difference is that in the catalyst the number of molybdenum neighbours surrounding each Mo ion is, on average, less than 6, the value in pure MoS_2. This indicates that the proportion of surface Mo ions is substantial and that the MoS_2 particles on the support surface contain only about 7–10 Mo atoms [5]. Such a small number of Mo atoms per average MoS_2 particle is in agreement with an electron microscopy study which showed that a large part of the MoS_2 material is present in the form of very small particles which are too small to be observed by electron microscopy [6].

Sulfided Co—Mo/Al_2O_3 and Ni—Mo/Al_2O_3 catalysts have a substantially higher catalytic activity than Mo/Al_2O_2, Co/Al_2O_3 or Ni/Al_2O_3 catalysts, and are therefore the catalysts of choice in industrial hydrotreating. This raises the question of what is the role of the Mo and Ni or Co atoms. Are the Mo surface atoms the catalytically active sites, and do the Ni (or Co) atoms have a beneficial effect on them, and should they therefore be called promoter atoms, or are the Ni atoms instead of the Mo atoms the active sites? Since pure molybdenum sulphide is much more active in hydrotreating reactions than pure nickel sulphide, over the years Mo had been thought to be the active component and Ni (or Co) the promoter. However, in a study of carbon-supported catalysts it was shown that a sulfided Ni/C catalyst can be as active as a Ni—Mo/C catalyst, and therefore Ni was proposed to be the active component [7,8]. To answer the question whether nickel is a promoter or a catalyst, information about the geometrical structure of Ni in the catalyst is needed.

The structure of the cobalt and nickel atoms was solved with the aid of inverse Mössbauer [9], EXAFS [10–12] and IR [13] spectroscopy. In the sulfidic form, nickel may be present in three forms, as Ni_3S_2 crystallites on the support surface, as nickel ions adsorbed on the edge surface of MoS_2 crystallites (the so-called Ni—Mo—S phase), and in octahedral sites in the γ-Al_2O_3 lattice. By combining Mössbauer and catalytic activity studies, Topsøe and coworkers established that the promoter effect of Co and Ni is related to the cobalt or nickel atoms in the Co—Mo—S and Ni—Mo—S phase, respectively [14]. Mössbauer [9] and IR studies [13] had indicated that the Co and Ni atoms are located at the edges of the MoS_2 crystallites, the exact location could be determined by EXAFS studies. They showed that in supported sulfided Ni—Mo catalysts the Ni atoms are surrounded by five sulfur atoms at 2.22 Å, one or two Mo atoms at 2.8 Å, and by one Ni atom at 3.2 Å [11]. These data are fully consistent with a model in which the Ni ions are located at the MoS_2 edges in the Mo plane in a square pyramidal coordination. The Ni ions are connected to the MoS_2 by four sulfur atoms, and the fifth sulfur atom is in the apical position in front of the Ni ion. A neighbouring Ni atom is located at the next edge position at 3.2 Å (*cf.* Fig. 1).

In the Ni—Mo catalysts all Mo atoms proved to be completely surrounded by six sulfur atoms, while in Mo-only catalysts the Mo atoms have a lower coordination number [12]. This shows that the Ni atoms and the sulfur atoms, which because of stoichiometry come together with the Ni atoms, fully cover the Mo atoms in the Ni—Mo catalysts. Since fully covered Mo atoms have no free ligand positions available to accommodate substrate molecules, the HDN reactions cannot take place at the Mo atoms in the Ni—Mo/Al_2O_3 catalysts. Therefore, the real catalytic sites in the Ni—Mo/Al_2O_3 catalysts are the Ni atoms, and the MoS_2 crystallites function as secondary support for these Ni atoms, the MoS_2 crystallites in turn being supported by the Al_2O_3 support.

Phosphate is frequently added to the catalyst impregnation solution to enhance the solubility of Mo. In addition, phosphate reacts with the Al_2O_3 support to $AlPO_4$ and decreases the support surface area [15–17]. As a consequence, the MoS_2 dispersion is diminished. Electron microscopy showed that the MoS_2 crystallites are indeed somewhat larger than in a phosphate-free catalyst and have a higher degree of stacking [18]. While the MoS_2 slabs at the MoS_2–Al_2O_3 interface can be modified by Mo—O—Al bonds with the support, the other MoS_2 slabs on top cannot

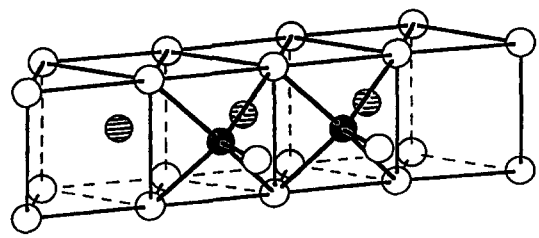

Fig. 1. Structure of the Ni atoms at the MoS_2 edge (white spheres S, black spheres Ni, striped spheres Mo).

have such bonds and will therefore be fully sulfided. Because of this difference in chemical composition, single slabs and slabs at "the bottom" of a stack may have different chemical properties than the "upper" MoS_2 slabs in a stack [19]. This has been used to explain the difference in hydrotreating activities between phosphate-modified and phosphate-free Ni—Mo catalysts [20].

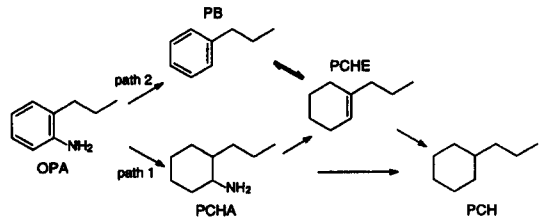

Fig. 3. HDN reaction network of ortho-propylaniline.

HDN OF ANILINE

Mechanism of the HDN of propylaniline

As shown in Fig. 2, the main products of the HDN of *o*-propylaniline (OPA) are propylcyclohexene (PCHE), propylbenzene (PB), and propylcyclohexane (PCH) [21,22]. Small amounts of *o*-propylcyclohexylamine (PCHA) were observed at short space times, suggesting that the first step in the HDN of OPA is the hydrogenation of OPA to PCHA. One reaction pathway in the HDN of OPA over sulfided $NiMo(P)/Al_2O_3$ catalysts would then be the hydrogenation of the phenyl group to form PCHA, followed by elimination of NH_3 to PCHE, and subsequent reaction to PB and PCH (path 1 in Fig. 3). Sulfided NiMo catalysts are perfectly capable of hydrogenating olefins and aromatics, and removal of the nitrogen atom from an aliphatic C—N fragment can, according to classic organic chemistry, take place *via* elimination. In the Hofmann elimination reaction, an acid helps in quaternizing the nitrogen atom and thereby creating a better leaving group, while a base promotes the elimination by removal of a β H atom (*cf.* Fig. 4).

Evidence for the existence of Brønsted acid sites in sulfided Mo, Co—Mo, and Ni—Mo catalysts has been presented [23], and it has indeed been shown that the removal of NH_3 from aliphatic amines with hydrogen atoms on the carbon atoms in the β position is easy, and that the rate is higher for molecules with more β H atoms [24]. Thus, the HDN rate of *t*-pentylamine is higher than that of pentylamine at 523 K, and that of 2,6-dimethylpiperidine is higher than that of piperidine at 548 K, while the HDN rate of neopentylamine (which has no β H atoms) is negligible under those conditions.

An HDN study of *o*-methylcyclohexylamine showed that this aliphatic amine was almost exclusively denitrogenated over sulfided $NiMo/Al_2O_3$ by elimination to methylcyclohexene [25], and confirmed that the HDN of OPA predominantly goes *via* hydrogenation to PCHA. Furthermore, co-reaction of ethylbenzene and OPA showed that even at high space time, hydrogenation of aromatics hardly occurred in the presence of OPA [22]. This demonstrates that the majority of the propylcyclohenxene observed in the HDN of OPA has not been formed by hydrogenolysis of OPA, followed by hydrogenation of the resulting benzene (path 2 in Fig. 3), but by hydrogenation of OPA, followed by elimination of NH_3 from PCHA (path 1 in Fig. 3).

Although it is clear that the main route for the HDN of OPA is through hydrogenation followed by elimination, the derivatives of the PB and PCH yields at low OPA conversion seem to be non zero (Fig. 2), suggesting that direct routes to PB and PCH do exist.

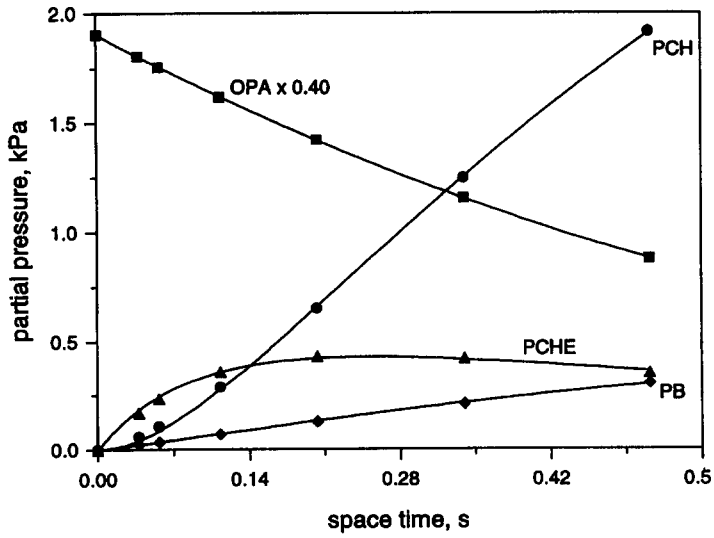

Fig. 2. Product composition vs space time in the HDN of OPA over $NIMoP/Al_2O_3$ at 623 K and 3.0 MPa.

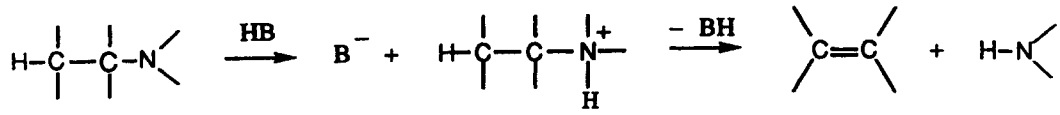

Fig. 4. Hofmann elimination of NH_3 from an amine.

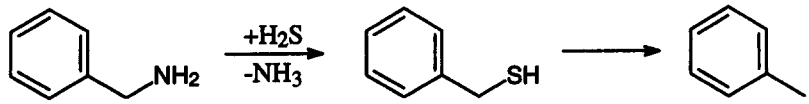

Fig. 5. Nitrogen removal from benzylamine by substitution of the NH_2 group of SH, and C—S bond hydrogenolysis.

Hydrogenolysis of the C—S bond is the dominant route for the hydrodesulfurization of thiophenol, but the C—N bond in aniline is much stronger and hydrogenolysis should be less important, although not impossible. This could explain a small direct contribution to the formation of PB. The direct formation of PCH and OPA is impossible, but could be visualised as the reaction from OPA to PCHA and on to PCH (*cf.* Fig. 3). If the PCHA intermediate reacts much faster than it is formed, its concentration will be very low and a direct reaction from PCHA to PCH would manifest itself as if a direct path from OPA to PCH were possible.

Indeed, deamination of alkylamines is not only possible through NH_3 elimination, but also through direct deamination. Thus, amines which have no hydrogen atoms on carbon atoms in the β position relative to the nitrogen atom can still be denitrogenated, albeit at a higher temperature. For instance, benzylamine was completely denitrogenated to toluene at 623 K [26]. The fact that no methylcyclohexane was formed demonstrates that hydrogenation of benzylamine to the corresponding aliphatic cyclohexylmethylamine (which is the thermodynamically stable product under these conditions), followed by elimination of NH_3 is slower than a direct removal of NH_3. This direct NH_3 removal can be explained by nucleophilic substitution of the amine group in benzylamine by a sulfhydryl group, followed by hydrogenolysis of the C—S bond (which is known to be relatively easy [27,28]) (Fig. 5). The alternative explanation, direct hydrogenolysis of the alkylamine to the hydrocarbon and NH_3 (Fig. 6) does not seem likely because of the positive effect of H_2S on C—N bond breaking. Therefore, the term hydrogenolysis should be avoided when describing C—N bond breaking, unless hydrogenolysis has really been proven mechanistically.

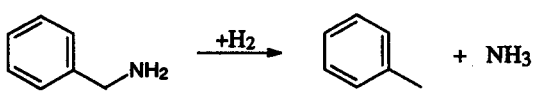

Fig. 6. Hydrogenolysis of the C—N bond in benzylamine.

Kinetics of the HDN of propylaniline

A kinetic study of the HDN of OPA was performed to determine which steps in the network of Fig. 3 are most important, and how the various reaction steps depend on the catalyst composition. Therefore, Mo/Al_2O_3 and $NiMo/Al_2O_3$ catalysts, with and without phosphate, were studied.

The number of kinetic parameters in the network of Fig. 3 is large: there could be 7 independent rate constants k_i, and 6 adsorption constants K_i for the reactant, intermediates and products (inclusive of NH_3). Several of these parameters are insignificant, however. For instance, the concentration of PCHA was always very low, so that the PCHA intermediate can be omitted from the kinetic analysis and PCHE can be considered as a primary HDN product, as demonstrated by Fig. 2. The reaction from PB to PCHE is insignificant, because of inhibitive adsorption of OPA. Furthermore, the adsorption constants of the hydrocarbons PCHE, PB and PCH are negligible compared to those of OPA and NH_3. On the other hand, reactions which are chemically different may take place on different catalytic sites. This would mean that the number of adsorption constants is equal to the number of sites times two (for OPA and NH_3). The kinetic network of Fig. 3 can therefore be simplified to that of Fig. 7.

Although $C(sp^2)$—N bond cleavage may take place on a different catalytic site than hydrogenation, it was not possible to distinguish between the catalytic sites of paths 1 and 2 in the kinetic modeling of the HDN of OPA, because the $C(sp^2)$—N bond cleavage was usually below 10% of the total HDN conversion over $NiMo(P)Al_2O_3$ catalysts. Hydrogenation of olefins has, however, been demonstrated to take place on a different catalytic site than the ring opening and N-removal elimination reactions of piperidine and decahydroquinoline [29], and therefore different adsorption constants were assumed for these different

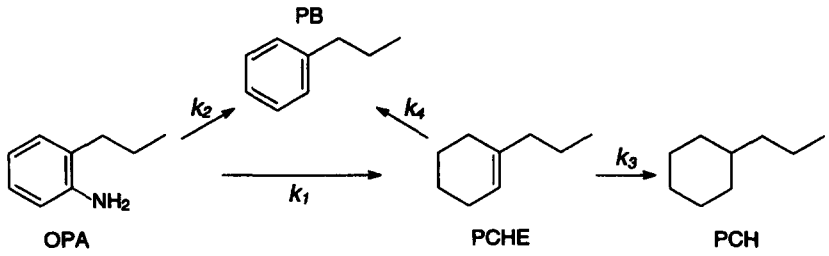

Fig. 7. Simplified kinetic network of the HDN of ortho-propylaniline.

sites. This leads to the following Langmuir–Hinshelwood rate equations:

$$\frac{dP_{OPA}}{dt} = -\frac{(k_1+K_2)K_{OPA}P_{OPA}}{1+K_{OPA}P_{OPA}+K_{NH_3}P_{NH_3}}, \quad (1)$$

$$\frac{dP_{PCHE}}{d\tau} = \frac{k_1 K_{OPA}P_{OPA}}{1+K_{OPA}P_{OPA}+K_{NH_3}P_{NH_3}} - \frac{(k_3+k_4)K_{PCHE}P_{PCHE}}{1+K'_{OPA}P_{OPA}+K'_{NH_3}P_{NH_3}}, \quad (2)$$

$$\frac{dP_{PB}}{d\tau} = \frac{k_2 K_{OPA}P_{OPA}}{1+K_{OPA}P_{OPA}+K_{NH_3}P_{NH_3}} + \frac{K_4 K_{PCHE}P_{PCHE}}{1+K'_{OPA}P_{OPA}+K'_{NH_3}P_{NH_3}}, \quad (3)$$

$$\frac{dP_{PCH}}{d\tau} = \frac{k_3 K_{PCHE}P_{PCHE}}{1+K'_{OPA}P_{OPA}+K'_{NH_3}P_{NH_3}}, \quad (4)$$

$$P_{NH_3} = P^0_{OPA} - P_{OPA}, \quad (5)$$

where τ is the space time, P_{OPA} and P_{NH_3} are the partial pressures of OPA and NH_3, respectively, in the reaction stream (P^0_{OPA} is the initial partial pressure of OPA), k_1 and k_2 are the HDN reaction rate constants through reaction paths 1 and 2 respectively (Fig. 7), K_{OPA} and K_{NH_3} are the Langmuir adsorption constants of OPA and NH_3 on the catalytic sites for the HDN reaction, and K'_{OPA} and K'_{NH_3} the adsorption constants of OPA and NH_3 on the catalytic site for olefin hydrogenation respectively, k_4 is the rate constant for the dehydrogenation of PCHE to PB, and k_3 and K_{PCHE} are the rate and adsorption constants of hydrogenation of PCHE and PCH, respectively.

Simulation of the experimental partial pressure against space time results of the HDN of OPA (Fig. 2) with these equations, with four rate constants and four adsorption constants (two for OPA and NH_3 on each site), did not give unique parameter values. Even if one of the parameters was varied over a large range, the other parameters could adapt reasonably well and the resulting fit was still acceptable. Apparently, the data were too much correlated to allow a unique solution of the kinetic parameters. Therefore, some of these parameters had to be determined by additional independent kinetic experiments, before the remaining parameters could be uniquely determined by fitting of the P-τ results presented in Fig. 2.

Instead of varying the space time, the initial partial pressure of the OPA reactant can be varied. At low OPA conversion, eq. (1) leads to:

$$-\ln(1-x_{OPA}) = \frac{(k_1+k_2)K_{OPA}}{1+K_{OPA}P^0_{OPA}}\cdot\tau. \quad (6)$$

By measuring x_{OPA}, the conversion of OPA, at a fixed space time as a function of the initial partial pressure of OPA, the sum of the rate constants k_1+k_2 and the adsorption constant K_{OPA} can be determined. Since $x_{PB} = k_2/(k_1+k_2)x_{OPA}$, the individual values of k_1 and k_2 can be obtained in combination with the initial slope of the x_{PB} (conversion to PB) vs x_{OPA} plot which gives the ratio of k_2/k_1 [30], once the sum of k_1+k_2 is known.

The kinetic parameters for the olefin hydrogenation reaction step (PCHE → PCH) in the HDN of the OPA (Fig. 7) can be determined by letting cyclohexene (CHE) react together with NH_3 or OPA under HDN reaction conditions. The inhibition adsorption constants of NH_3 or OPA on this hydrogenation reaction can be obtained with the aid of eq. (7):

$$-\ln(1-x_{CHE}) = \frac{k_{CHE}K_{CHE}}{1+K'_iP_i}\cdot\tau \quad (7)$$

where K'_i is the adsorption constant of the inhibitor on the olefin hydrogenation site, and P_i is the partial pressure of the inhibitor in the reaction stream.

Once the HDN rate constants k_1 and k_2, and the adsorption constant K_{OPA} of the OPA on the HDN site, and the adsorption constants K'_{OPA} and K'_{NH_3} of OPA and NH_3 on the hydrogenation site are known, the partial pressure against space time results (Fig. 2) can be fitted with the Langmuir–Hinshelwood equations given in eqs (1)–(5) to determine the constants k_3K_{PCHE}, k_4K_{PCHE} and K'_{NH_3}. Because now only three parameters have to be fitted, the confidence ranges are quite narrow and the confidence levels high. The results of the fitting for $NiMoP/Al_2O_3$ are given in Fig. 2.

Table 1 gives the values of the rate and adsorption constants over the Mo/Al_2O_3, MoP/Al_2O_3, NiMo-P/Al_2O_3 and $NiMoP/Al_2O_3$ catalysts at 623 K and 3 MPa. The 95% confidence range of the rate and

Table 1. Kinetic parameters of the HDN network of OPA at 623 K, 3.0 MPa and P_{H2S} = 6.5 kPa over different catalysts (k in kPa s^{-1} and K in kPa^{-1})

Parameters	Mo/Al_2O_3	MoP/Al_2O_3	$NiMo/Al_2O_3$	$NiMoP/Al_2O_3$
k_1	0.8	0.8	5.8	6.4
k_2	0.2	0.3	0.4	0.8
k_3K_{PCHE}	7.6	6.2	38	48
k_4K_{PCHE}	0.9	1.2	1.1	1.4
K_{OPA}	0.3	0.5	0.7	1.2
K_{NH_3}	0.4	0.4	0.5	1.0
K'_{OPA}	0.2	0.3	0.4	0.9
K'_{NH_3}	0.4	0.6	0.5	1.0

K_i relate to the conversion of OPA, and K'_i to the alkene hydrogenation.

adsorption constants were usually within 10% and 20% of the parameter values, respectively. The results show that the $NiMo/Al_2O_3$ and $NiMo/Al_2O_3$ catalysts have a low PB selectivity (7–12%), while the Mo/Al_2O_3 and MoP/Al_2O_3 catalysts produce about 30% PB. The ratios k_4/k_3 and k_2/k_1 demonstrate that direct C(sp^2)—N bond cleavage of OPA is the main route for PB production at all temperatures and for all catalysts.

Introduction of phosphorus to a $NiMo/Al_2O_3$ catalyst increases the reaction rate constants k_1 and k_2 of HDN paths 1 and 2 (Fig. 7), as well as the adsorption constants of OPA. The resulting effective rate constants $(k_1+k_2)K_{OPA}/(1+K_{OPA}P^0_{OPA})$ are higher over the P-containing catalyst which accounts for the promotional effect of phosphorus over the $NiMoP/Al_2O_3$ catalyst.

The results presented in Table 1 also clearly demonstrate that OPA adsorbs with a different strength on the catalytic site for the HDN of OPA as on the site for the hydrogenation of CHE, even though the rate-limiting reaction step in both cases is a hydrogenation reaction. In the first case the phenyl group of aniline is involved and in the second case an alkene group. This indicates that the catalytic site for the hydrogenation of the phenyl group in aniline is different from that for the hydrogenation of an olefin.

In the presence of OPA and NH_3, the effective rate constant $(k_{CHE}K_{CHE}/(1+K'_iP_i)$ of the hydrogenation reaction was lower over the $NiMoP/Al_2O_3$ catalyst, demonstrating that phosphorus has a negative effect on the hydrogenation of CHE. In the absence of these nitrogen-containing compounds, however, phosphorus has a promotional effect (Table 2). This shows that the negative effect of phosphorus on the hydrogenation of an olefin in the presence of nitrogen-containing compounds is not due to the intrinsic kinetics, but to the higher adsorption constants of the nitrogen-containing compounds over the $NiMo(P)/Al_2O_3$ catalyst relative to the $NiMo/Al_2O_3$ catalyst and thus to a stronger inhibition of the olefin hydrogenation. Although the HDN of OPA and hydrogenation of CHE take place on different catalytic sites, OPA adsorbs on the catalytic site for the hydrogenation of CHE as well and hinders this hydrogenation reaction. The same effect was observed in the hydrogenation of ethylbenzene (Table 2).

Table 2. Comparison of the effective rate constants (in s^{-1}) of the hydrogenation of ethylbenzene (EB) and cyclohexene (CHE) at 593 K and 3.0 MPa

	P_{H_2S} = 6.5 kPa		P_{H_2S} = 0	
Catalyst	$k_{CHE}K_{CHE}$	$k_{EB}K_{EB}$	$k_{CHE}K_{CHE}$	$k_{EB}K_{EB}$
$NiMo/Al_2O_3$	16	0.04	69	0.2
$NiMoP/Al_2O_3$	22	0.06	98	0.4

For the Mo/Al_2O_3 and MoP/Al_2O_3 catalysts, a small contribution from a direct route from OPA (*via* PCHA) to PCH had to be added to the rate equations in order to obtain a good fit of the experimental data at small space time. For the $NiMo/Al_2O_3$ and $NiMoP/Al_2O_3$ catalysts, the addition of this route did not improve the quality of the fit. It thus looks as if the Mo-only (Ni free) catalysts are capable of hydrolyzing the C—N bond in OPA, as well as in PCHA. Further work is needed to establish how fast the direct hydrogenolysis of PCHA really is relative to the elimination reaction.

Implications for the catalytic sites

Neither the activation energies of the HDN reaction paths 1 and 2, nor the heats of adsorption of OPA on the catalytic sites for HDN and hydrogenation showed any difference between the $NiMo/Al_2O_3$ and $NiMoP/Al_2O_3$ catalysts (Table 3) [22]. This suggests that phosphorus does not change the catalytic sites for the HDN of OPA, but increases their number. Apparently, phosphorus does not participate directly in the HDN reaction, but only indirectly. Phosphorus is present as phosphate in the catalysts. Some of this phosphate might be reduced to PH_3 by spilled-over hydrogen atoms, and this PH_3 might induce an exchange of surface S^{2-} by P^{3-} anions [30,32], thus

Table 3. Activation energies in paths 1 and 2, and heats of adsorption of OPA on the HDN and hydrogenation (HG) sites in the HDN of OPA at 3.0 MPa and $P_{H_2S} = 6.5$ kPa

	E (kJ/mol)		$-\Delta H_{ad}$ (kJ/mol)	
Catalyst	Path 1	Path 2	HDN site	HG site
$NiMo/Al_2O_3$	174	122	70	42
$NiMoP/Al_2O_3$	171	117	68	44

creating more surface anion vacancies because of the charge difference between S^{2-} and P^{3-}. In this way, more coordinatively-unsaturated Ni and or Mo surface atoms at the edges and corners of the Ni—MoS_2 crystallites, which are the active sites for hydrotreating reactions [1,2], are created. On the other hand, the stacking of the MoS_2 slabs may also be increased by the introduction of phosphorus in a sulfided NiMo (P)/Al_2O_3 catalyst [18,35] which may lead to different amounts of rim, edge, and basal sites, and thus to different reactivities as proposed by Daage and Chianelli [19].

The heats of adsorption of OPA and NH_3 were much higher over the HDN site than over the olefin hydrogenation site (Table 3). This confirms that different sites are responsible for the hydrogenation of an olefin group and of the phenyl group in an aniline molecule. By modifying the ratio of these sites, it should therefore, in principle, be possible to modify the selectivity of a catalyst toward different reactions.

Table 1 shows that the presence of nickel increases the rate constant k_1 of reaction path 1 (which is rate limited by hydrogenation of the phenyl group of aniline) as well as that (k_2) of reaction of path 2, the C(sp^2)—N bond cleavage. The rate constant of hydrogenation increased by a factor of $6 \sim 7$, and that of the C(sp^2)—N bond cleavage by a factor of $2 \sim 3$. A similar increase by a factor of $5 \sim 8$ is observed in the parameter $k_4 K_{PCHE}$ of the hydrogenation of PCHE. In the absence of nickel, k_1 is the same over Mo/Al_2O_3 and MoP/Al_2O_3 catalysts, suggesting that the number and/or the intrinsic activity of the phenyl hydrogenation site are not influenced by the presence of phosphorus. The adsorption constant of OPA, on the other hand, was increased by the presence of phosphorus. Therefore, the promotional effect of phosphorus over Mo/Al_2O_3 catalysts in the HDN of OPA is only due to the favourable adsorption of reactant over the phosphorus-containing catalysts.

C—N bond cleavage is an indispensable step in the HDN process, which usually takes place through saturated amine intermediates. Our kinetic results confirm that the majority of the C—N bond cleavage in the HDN of OPA takes place through C(sp^3)—N bond cleavage of PCHA. There can be two ways of C(sp^3)—N bond cleavage: elimination and hydrogenolysis. By studying a series of amines, Portefaix *et al.* demonstrated that an E2 Hofmann type elimination mechanism is responsible for the C—N bond cleavage in molecules which contain hydrogen atoms in the β-C position [24]. In our case, the reaction of PCHA to PCHE is an elimination and the reaction of PCHA to PCH a hydrogenolysis. Elimination is the main route for C—N bond cleavage in propylaniline as well: only $20 \sim 30\%$ of the C—N bond cleavage takes place through hydrogenolysis over the Mo/Al_2O_3 and MoP/Al_2O_3 catalysts, and even less (10%) over the $NiMo/Al_2O_3$ and $NiMoP/Al_2O_3$ catalysts [22].

HDN OF DECAHYDROQUINOLINE

Decahydroquinoline (DHQ) is a representative of the second class of molecules with a specific HDN mechanism. Like piperidine it contains a nitrogen-containing ring which does not have to be hydrogenated before denitrogenation as the phenyl group in aniline. Its advantage over piperidine is that it hardly forms any by-products by disproportionation of two DHQ molecules, or through addition of DHQ to the HDN product PCHE. Such by-products (as N-pentylpiperidine in the case of piperidine) not only complicate the analysis of the product mixture, but also the data analysis. On the other hand, the second ring in DHQ makes the study of its HDN more difficult than that of OPA, because not only HDN reactions take place, but also dehydrogenation reactions of DHQ to 1,2,3,4-tetrahydroquinoline (THQ1) and 5,6,7,8-tetrahydroquinoline (THQ5). The latter two molecules may even react further to quinoline and OPA and open an additional HDN channel (as described in the foregoing section). By performing the HDN of DHQ at 623 K, 3.0 MPa and low space times, the dehydrogenation of DHQ to THQ1 and of THQ5 to Q could be kept at a low level. As a consequence, the further reaction of THQ1 or OPA was insignificant and the reaction network could be simplified as in Fig. 8.

The HDN conversion of DHQ as a function of space time (Fig. 9) demonstrated that propylcyclohexylamine (PCHA) is a primary product. Cis- as well as trans-PCHA could be detected and shown to be the reaction intermediates between cis- and trans-DHQ and PCHE [29]. The amount of PCHE formed indicated that most of the HDN reaction of PCHA proceeds through elimination of ammonia rather than by hydrogenolysis. Nevertheless, the direct product (allylcyclohexylamine) of the elimination reaction of NH_3 from DHQ was not observed, probably due to its strong adsorption and fast hydrogenation to PCHA.

The HDN results at low space time suggested that PCH is a primary product as well, and a good fit of the kinetic results could only be obtained when a direct path from DHQ to PCH was included. Such an apparent double hydrogenolysis reaction does not make much chemical sense, but can be explained by

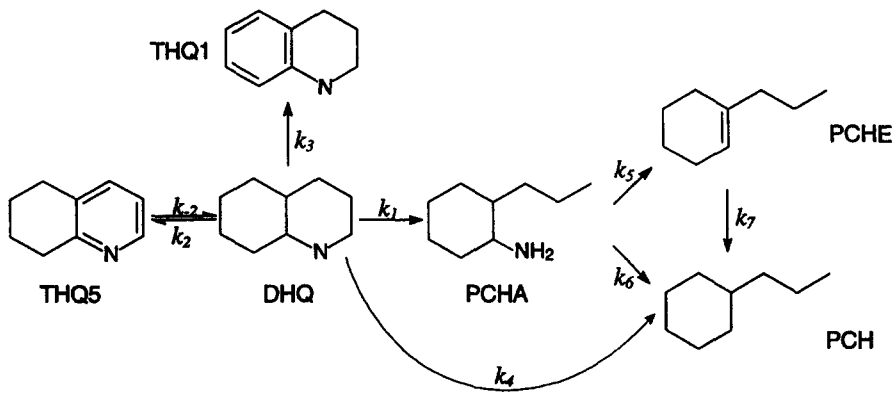

Fig. 8. Reaction network of the HDN of decahydroquinoline (DHQ).

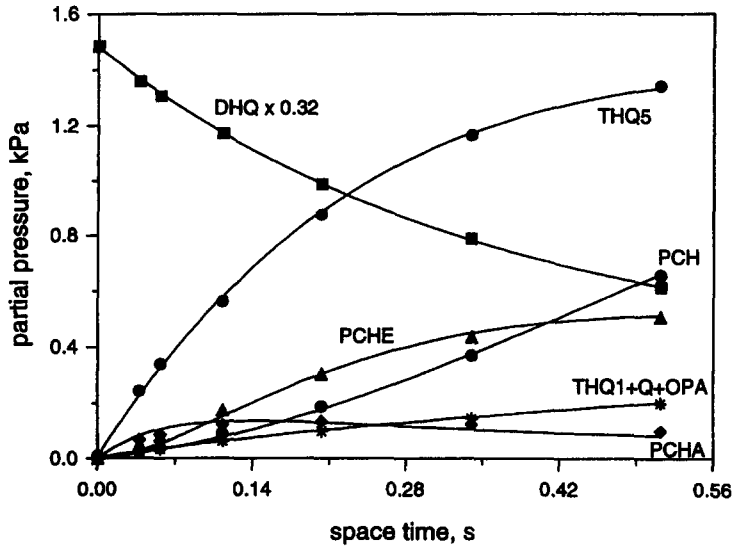

Fig. 9. Product composition vs space time in the HDN of DHQ over $NiMoP/Al_2O_3$ at 623 K and 3.0 MPa.

diffusion limitations. Since k_5K_{PCHA}, k_6K_{PCHA} and k_7K_{PCHE} are large and k_1K_{DHQ} is small (Table 4), it might well be that as soon as the PCHA and PCHE intermediates are formed at the catalytically active surface inside the catalyst pores, they react very quickly to the final PCH product before being able to diffuse out of the pores. In that case, the experimentally observed concentrations outside the pores underestimate the concentrations of the PCHA and PCHE intermediates and overestimate the PCH product concentration in the pores. Mathematically this manifests itself as an apparent direct path of reactant DHQ to product PCH. Additional studies should resolve the question if the DHQ to PCH path is real or apparent.

The kinetic parameters in the HDN network of DHQ were determined just as described in the foregoing section for the parameters in the HDN network of OPA. The results obtained at 623 K and 3.0 MPa are presented in Table 4 and a comparison between experimental results and fits for the $NiMoP/Al_2O_3$ catalyst is shown in Fig. 9.

Introduction of Ni increased the rate constant k_1 of the first elimination step by a factor of $2 \sim 3$, and the effective rate constant k_7K_{PCHE} of the olefin hydrogenation by a factor of $5 \sim 7$ (Table 4). In the forgoing section on the HDN of OPA it was found that Ni improved the rate determining hydrogenation of the phenyl group of OPA by a factor of $6 \sim 7$. It is clear that Ni increases all reaction rates, but hydrogenation rates more than elimination rates. The explanation for the weaker influence of Ni on the elimination reaction might be that for elimination not only a Lewis acid metal ion site (Mo^{4+} or Ni^{2+}) but also a basic S^{2-} or SH^- site is required. The properties of this basic site should be only weakly dependent on the metal ion present. The similarity of the adsorption constant of DHQ on the site for its ring opening elimination for all four catalysts (Table 4) also suggests that the elimination is primarily determined by the presence of S^{2-} or SH^- and only secondarily by that of Mo, Ni or P.

Introduction of phosphorus to a $NiMo/Al_2O_3$ catalyst in the presence of H_2S decreases the rate constant of the first C—N bond cleavage (which is the rate limiting step in the HDN of DHQ), but changes the adsorption constant of DHQ only slightly (Table 4).

Table 4. Kinetics parameters of the HDN network of DHQ at 623 K, 3.0 MPa and P_{H_2S} = 6.5 kPa over different catalysts (k in kPa s^{-1} and K in kPa^{-1})

Parameters	Mo/Al_2O_3	MoP/Al_2O_3	$NiMo/Al_2O_3$	$NiMoP/Al_2O_3$
k_1	1.9	1.5	5.1	4.6
k_2	7.5	7.8	11	11
k_{-2}	10		14	13
k_3	0.5	0.5	0.9	1.0
k_4	0.8	0.8	1.0	0.8
k_5K_{PCHA}	50	51	48	47
k_6K_{PCHA}	10	4	4	4
k_7K_{PCHE}	5	6	27	41
k_{DHQ}	0.2	0.4	0.4	0.4
k_{THQ5}	0.1	0.2	0.3	0.3
K_{NH_3}	0.1	0.3	0.3	0.3
K'_{DHQ}	0.2	0.3	0.2	0.3
K'_{NH_3}	0.1	0.15	0.1	0.15
K''_{DHQ}	0.8	0.9	1.6	3.5
K''_{NH_3}	0.4	0.6	0.5	1.0

K_i relate to the reaction of DHQ to PCHA, K'_i to the reaction of DHQ to THQ5, and K''_i to the alkene hydrogenation.

As a result, the effective rate constant $k_1K_{DHQ}/(1+K_{DHQ}P^0_{DHQ})$ of the first C—N bond cleavage (rate limiting step) is lower for the $NiMoP/Al_2O_3$ than for the $NiMo/Al_2O_3$ catalyst, explaining why phosphorus has a negative effect on the HDN in the presence of H_2S. The lower rate constant and unaltered adsorption constant suggest that phosphorus decreases the number of elimination sites. Phosphorus decreases the surface area and pore volume of the support [31], and might therefore decrease the dispersion of the NiMoS phase as well.

The adsorption constant of DHQ on the site for the reaction of DHQ to PCHA is much smaller than the adsorption constant which describes its inhibition effect in the hydrogenation of CHE. The fact that one and the same molecule has different adsorption constants for different reactions confirms that different catalytic sites are involved in these chemically different reaction steps in the HDN network. This is supported by the observation that H_2S promotes the C—N bond cleavage reaction of DHQ, while it inhibits the hydrogenation of alkenes [29]. Therefore, one and the same catalytic site cannot be responsible for these different reaction steps in the HDN kinetic studies.

HDN OF QUINOLINE

Quinoline (Q) has often been used as a model compound in hydrodenitrogenation [34], because it has many advantages over other nitrogen-containing hydrocarbons. Due to its bicyclic molecular structure, all reactions which take place in industrial HDN occur in the HDN reaction network of quinoline as well, for instance C—N bond cleavage, hydrogenation of an aromatic heterocyclic ring, and hydrogenation of a phenyl ring. The reaction mechanism of quinoline HDN has been studied by several groups [20,28,34–37], and has also been reviewed a few times [21,38,39]. It is generally accepted that the HDN mechanism through the intermediates indicated in the reaction network presented in Fig. 10. In principle, there are two ways to remove the nitrogen atom from quinoline, *via* OPA or *via* DHQ. In the first path, the heterocycle in quinoline (Q) is hydrogenated to 1,2,3,4-tetrahydroquinoline (THQ1) followed by ring opening to OPA. OPA is subsequently hydrogenated to PCHA, and the nitrogen atom is removed from PCHA by elimination as we have seen in the Aniline Section. In the second HDN path, quinoline is fully hydrogenated to DHQ which then reacts to PCHA and on to hydrocarbons, as described in the Decahydroquinoline Section.

The effects of Ni, H_2S and phosphorus on the HDN of quinoline can be understood by considering the effects on the two pathways. Since Ni promotes the HDN and DHQ as well as that of OPA, it is no surprise that $NiMo/Al_2O_3$ is a better catalyst for the HDN of quinoline that Mo/Al_2O_3 under all conditions. Addition of H_2S leads to a higher HDN for Q as well as DHQ, but to a lower HDN for OPA (Table 5), and indicates that the major contribution to the HDN of Q is through the DHQ-PCHA reaction path. The reason for the different influence of H_2S on DHQ and OPA is that in the case of the HDN of DHQ the rate determining step is the ring opening of DHQ through elimination which runs faster on a fully sulfided catalyst surface (and is thus promoted by the presence of H_2S), while the rate determining step in the HDN of OPA is the hydrogenation of OPA to PCHA which runs faster on a sulfur-poor catalyst surface (and is thus poisoned by the presence of H_2S).

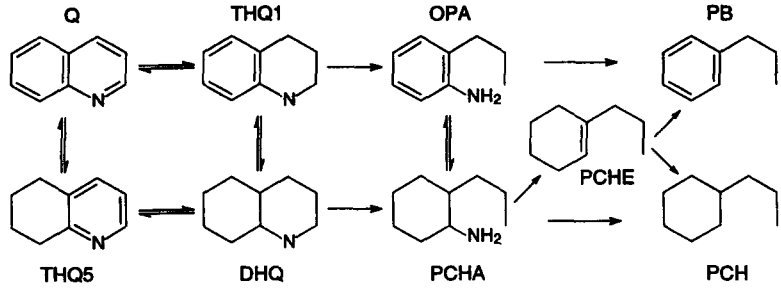

Fig. 10. Reaction network of the HDN of quinoline (Q).

Table 5. Yields of hydrocarbons (%) in the HDN of quinoline, decahydroquinoline, piperidine and *o*-propylaniline at 3.0 MPa in the presence (+) and absence (−) of 6.5 kPa H_2S

Catalyst	T (K)	Q		DHQ		Pip		OPA	
		+	−	+	−	+	−	+	−
$NiMo/Al_2O_3$	643	26	9	47	20			84	90
$NiMoP/Al_2O_3$	643	32	21	49	34			100	100
$NiMo/Al_2O_3$	623	15	5	46	13	81	10	64	76
$NiMoP/Al_2O_3$	623	18	9	43	22	67	10	91	96
$NiMo/Al_2O_3$	593	3	1	20	4	48	6	24	37
$NiMoP/Al_2O_3$	593	5	2	16	5	37	6	35	53

In agreement with this explanation, the HDN of the monocyclic piperidine was also promoted by the presence of H_2S (Table 5).

Phosphorus exhibits a promotional effect on the HDN of OPA, both in the presence and absence of H_2S, and on that of DHQ in the absence of H_2S (Table 5). In the presence of H_2S, however, the effect of phosphorus on the HDN and DHQ is complex. At 593 and 623 K it is negative, like that on the HDN of piperidine, while at 643 K it is weakly positive. The effect of phosphorus on the HDN of Q is positive at all temperatures, in the presence as well as in the absence of H_2S. This shows that the THQ1-OPA path is responsible for the promoting effect of phosphorus in the HDN of Q.

H_2S and P have opposite effects: H_2S promotes the HDN path *via* DHQ, because it promotes the rate determining reaction of DHQ or PCHA. At the same time, it inhibits the OPA pathway, because it retards the rate determining hydrogenation of OPA. The effect of P is just opposite: it increases the rate of OPA to PCHA and decreases the rate of DHQ to PCHA in the presence of H_2S below 643 K (the small increase at 643 K will be discussed below). Because the H_2S effect is the stronger of the two, the result of the combined presence of H_2S and P is a higher total HDN conversion of Q. In the absence of H_2S, the contribution of the DHQ-PCHA path is suppressed and the contribution of the THQ1-OPA remains more or less constant, because a slower transformation of THQ1 to OPA is compensated by an increased transformation of OPA to HC. Since phosphorus promotes the HDN of OPA strongly, a strong promotional effect of phosphorus is observed on the HDN of Q in the absence of H_2S. The rate-limiting reaction step of the THQ1-OPA path may even be shifted from the conversion of OPA in the presence of H_2S to the formation of OPA from THQ1 in the absence of H_2S.

The negligible effect of phosphorus on the HDN of piperidine in the absence of H_2S suggests that phosphorus should have an equally small effect in the HDN and DHQ. However, Table 5 shows that phosphorus promotes the HDN of DHQ in the absence of H_2S. This suggests that not only Q, but also DHQ can be hydrodenitrogenated *via* THQ1 and OPA (Fig. 11). The absence of H_2S and the presence of P are the best conditions for the dehydrogenation of DHQ to THQ1. The low OPA concentration and low PCH/PB ratio in the HDN of DHQ demonstrate that in the absence of H_2S part of DHQ indeed reacts *via* THQ1 and OPA. The higher the temperature, the more this path becomes important, because high temperatures favour the dehydrogenation of DHQ to THQ1. At the highest temperature, 643 K, the DHQ-THQ1-OPA route is even important in the presence of H_2S. At this temperature, the reactions between DHQ, THQ1, THQ5 and Q are so fast that a quasi equilibrium between these four components is established. Therefore, at 643 K the HDN of DHQ resembles that of Q very much, and is promoted by phosphorus *via* the THQ1-OPA path. The small change in the HDN conversion of DHQ when increasing the temperature

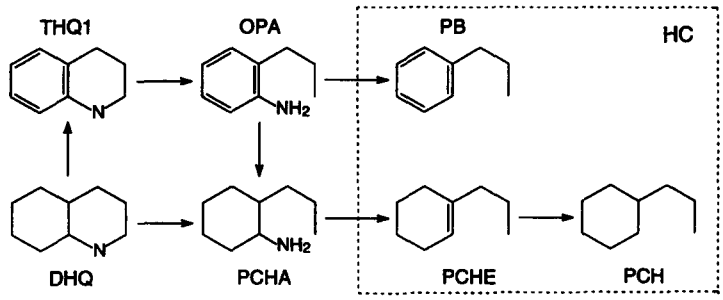

Fig. 11. Formation of hydrocarbons in the HDN of DHQ through PCHA as well as through THQ1 and OPA.

from 623 to 643 K (Table 5), further demonstrates that at higher temperature a new channel opens which takes away DHQ and limits the direct HDN conversion *via* PCHA to hydrocarbons.

The contribution of the DHQ-THQ1-OPA-HC pathway (Fig. 11) can be estimated from the amount of propylbenzene (PB) formed during the HDN reaction. The formation of PB from PCHE in the DHQ-PCHA-PCHE-HC pathway is completely inhibited by DHQ, and all PB produced in the HDN of DHQ must come from hydrogenolysis of OPA. The results show that about 40% of the HDN reaction of DHQ takes place through the reaction path DHQ-THQ1-OPA-HC in the absence of H_2S, but less than 10% in the presence of H_2S.

CONCLUSIONS

Removal of the nitrogen atom from aromatic nitrogen-containing molecules takes place *via* a sequence of reaction steps: hydrogenation of aromatic rings, NH_3 elimination and olefin hydrogenation. The separate reaction steps cannot be lumped together into one kinetic equation, because every reaction takes place on a different catalytic site which differs in its ability to bind reactants, intermediates and products. Depending on the type of molecule, aniline or pyridine-like, the rate determining step at 3.0 MPa and 593–643 K is hydrogenation or ring opening elimination, respectively.

The positive or negative effects of catalyst components are due to their influence on the rate and adsorption constants. The effective rate constants $kK/(1+KP)$ calculated for reactant partial pressures of 5 kPa (Table 6) show that Mo/Al_2O_3 and MoP/Al_2O_3 catalysts have about equally low rates, $NiMo(P)/Al_2O_3$ catalysts have higher rates than $Mo(P)/Al_2O_3$ catalysts for all reactants, and $NiMo\text{-}P/Al_2O_3$ catalysts have higher or lower rates than $NiMo/Al_2O_3$ catalysts, depending on the reactants. The effect of Ni is thus positive in all cases, and that of phosphorus depends on the reactant, that is on the type of rate determining reaction. Hydrogenation reactions are promoted by P (OPA and PCHE), and elimination reactions are negatively influenced (DHQ and Pip). The reverse is true for the influence of H_2S

The HDN behaviour of large aromatic N-containing molecules looks very complex at first sight. Once it is realised, however, that both classes of HDN reactions, of aniline and pyridine-like molecules, contribute to their HDN, the HDN behaviour becomes understandable. Thus, in the HDN of quinoline the reaction path *via* DHQ-PCHA is promoted by H_2S and negatively influenced by phosphorus, while the reverse is true for the path *via* THQ1-OPA. The former path results in a low PCH/PB, and the latter in a high PCH/PB product ratio. The promotional effect of phosphorus in the HDN of quinoline is determined by the THQ1-OPA path, and is due to an increased intrinsic rate constant for the hydrogenation of the phenyl group in OPA, indicating that it increases the number of the corresponding active sites of $NiMo/Al_2O_3$ catalysts. The influence of phosphorus addition is similar to that of omitting H_2S from the

Table 6. Effective rate constants $kK/(1+KP)$ (in s^{-1}) at 623 K, 3.0 MPa, $P_{H_2S} = 6.5$ kPa and $P_R = 5$ kPa over different catalysts

Reactant R	Mo/Al_2O_3	MoP/Al_2O_3	$NiMo/Al_2O_3$	$NiMoP/Al_2O_3$
DHQ	0.2	0.2	0.7	0.6
OPA	0.1	0.1	0.9	1.1
PCHE	5	6	27	41
PCHE+OPA	3.8	2.5	12.7	8.7
PCHE+DHQ	1	1.1	3	2.2

feed, suggesting that phosphorus increases the number of sulfur vacancies which are considered to be the catalytic sites for the (de)hydrotreating reactions.

REFERENCES

1. Knözinger, H., in *Proceedings of 9th International Congress Catalysis*, Vol. 5, ed. M. J. Phillips and M. Teman. The Chemical Institute of Canada, 1988, p. 20.
2. Prins, R., de Beer, V. H. J. and Somorjai, G. A., *Catal. Rev. Sci. Eng.*, 1989, **31,** 1.
3. Clausen, B. S., Topsøe, H., Candia, R., Villadsen, J., Lengeler, B., Als-Nielsen, J. and Christensen, F., *J. Phys. Chem.*, 1981, **85,** 3868.
4. Parham, T. G. and Merrill, R. P., *J. Catal.*, 1984, **85,** 295.
5. Bouwens, S. M. A. M., Prins, R., de Beer, V. H. J. and Koningsberger, D. C., *J. Phys. Chem.*, 1990, **94,** 3711.
6. Eijsbouts, S., Heinerman, J. J. L. and Elzerman, H. J. W., *Appl. Catal. A.*, 1993, **105,** 53.
7. Duchet, J. C., van Oers, E. M., de Beer, V. H. J. and Prins, R., *J. Catal.*, 1983, **80,** 386.
8. Vissers, J. P. R., de Beer, V. H. J. and Prins, R., *J. Chem. Soc., Faraday Trans.* 1, 1987, **83,** 2145.
9. Topsøe, H., Clausen, B. S., Candia, R., Wivel, C. and Mrup, S., *J. Catal.*, 1981, **68,** 433.
10. Clausen, B. S., Lengeler, B., Candia, R., Als-Nielsen, J. and Topsøe, H., *Bull. Soc. Chim. Belg.*, 1981, **90,** 1249.
11. Louwers, S. P. A. and Prins, R., *J. Catal.*, 1992, **133,** 94.
12. Bouwens, S. M. A. M., van Zon, F. B. M., van Dijk, M. P., van der Kraan, A. M., de Beer, V. H. J., van Veen, J. A. R. and Koningsberger, D. C., *J. Catal.*, 1994, **146,** 375.
13. Topsøe, N. Y. and Topsøe, H., *J. Catal.* 1983, **84,** 386.
14. Wivel, C., Candia, R., Clausen, B. S., Mrup, S. and Topsøe, H., *J. Catal.*, 1981, **68,** 453.
15. Lopez Cordero, R., Esquivel, N., Lazaro, J., Fierro, J. L. G. and Lopez Agudo, A., *Appl. Catal.*, 1989, **48,** 341.
16. DeCanio, E. C., Edwards, J. C., Scalzo, T. R., Storm, D. A. and Bruno, J. W., *J. Catal.*, 1991, **132,** 498.
17. Kraus, H., Prins, R. and Kentgens, A., *J. Phys. Chem.*, 1996, **100,** 16336; and 1995, **99,** 16080.
18. Ryan, R. C., Kemp, R. A., Smegal, J. A., Denley, D. R. and Spinnler, G. A., *Stud. Surf. Sci. Catal.*, 1989, **50,** 21.
19. Daage, M. and Chianelli, R. R., *J. Catal*, 1994, **149,** 414.
20. Eijsbouts, S., van Gestel, J. N. M., van Veen, J. A. R., de Beer, V. H. J. and Prins, R., *J. Catal.*, 1991, **131,** 412.
21. Schulz, H., Schon, M. and Rahman, N. M., *Stud. Surf. Sci. Catal.*, 1986, **27,** 201.
22. Jian, M., Kapteijn, F. and Prins, R., *J. Catal.*, in press.
23. Topsøe, N. Y., Topsøe, H. and Massoth, F. E., *J. Catal.*, 1989, **119,** 252.
24. Portefaix, J. L., Cattenot, M., Guerriche, M., Thivolle-Cazat, J. and Breysse, M., *Catal. Today*, 1991, **10,** 473.
25. Flechsenhar, M. and Prins, R., to be published.
26. Vivier, L., Dominquez, V., Perot, G. and Kasztelan, S., *J. Molec. Catal.*, 1991, **67,** 267.
27. Moreau, C., Joffre, J., Saenz, C. and Geneste, P., *J. Catal.*, 1990, **122,** 448.
28. Perot, G., Brunet, G., Canaff, C. and Toulhoat, H., *Bull. Soc. Chim. Belg.*, 1987, **96,** 865.
29. Jian, M. and Prins, R., *Stud. Surf. Sci. Catal.*, 1996, **101,** 87.
30. Jian, M. and Prins, R., *Catal. Today*, 1996, **30,** 127.
31. Jian, M. and Prins, R., *Catal. Letters*, 1995, **35,** 193.
32. Mangnus, P. J., van Langeveld, A. D., de Beer, V. H. J. and Moulijn, J. A., *Appl. Catal.*, 1991, **68,** 161.
33. Payen, E., Hubaut, R., Kasztelan, S., Poulet, O. and Grimblot, J., *J. Catal.*, 1994, **147,** 123.
34. Satterfield, C. N. and Gültekin, S., *Ind. Eng. Chem. Process Des. Dev.*, 1981, **20,** 62.
35. Satterfield, C. N. and Yang, S. H., *Ind. Eng. Chem. Process Des. Dev.*, 1984, **23,** 11 and 20.
36. Gioia, F. and Lee, V., *Ind. Eng. Chem. Process Des. Dev.*, 1986, **25,** 918.
37. Perot, G., *Catal. Today*, 1991, **10,** 447.
38. Ho, T. C., *Catal. Rev. Sci. Eng.*, 1988, **30,** 117.
39. Girgis, M. J. and Gates, B. C., *Ind. Eng. Chem. Res.*, 1991, **30,** 2021.